Stability and Collapse of Metallic Structures on Surfaces

W. D. Luedtke and Uzi Landman
School of Physics, Georgia Institute of Technology, Atlanta, Georgia 30332
(Received 20 December 1993)

Energetics, structure, stability, and collapse mechanisms of adsorbed gold clusters on Ni(100) and Au(111) surfaces were investigated with molecular dynamics simulations. Settling and spreading of Au clusters on Ni(100), driven by gain in cohesion and aided by the large interfacial lattice mismatch, are linear in time and occur via diffusionless sequences of atomic embedments between layers of the adsorbed cluster. Enhanced stability of epitaxial Au clusters on Au(111) was observed, and their collapse at elevated temperatures occurs via a dislocation mediated settling mechanism.

PACS numbers: 68.35.Bs, 61.46.+w

Basic and technological interest in the physical properties of small materials structures, and in locally controlled surface modifications, underlie intensifying research endeavors in this area [1–3]. Using molecular dynamics (MD) simulations, we have explored the structure, energetics, dynamics, stability, and collapse mechanisms of surface-supported metallic nanostructures which are key issues in preparation, control, and exploitation of such structures.

We show that heterostructures, such as a three-dimensional (3D) crystalline gold cluster (dot) deposited on a Ni(100) surface, where the lattice mismatch is large (16%) and the surface energy of the nickel substrate is larger than that of the deposited Au dot, can collapse via a nondiffusional solid-on-solid settling (SOSS) mechanism. The SOSS involves a succession of layer-by-layer incorporations (embedment) of Au atoms from a given layer into the underlying Au layer, accompanied by subsequent cooperative stress relief via lateral displacements of atoms in the underlayer. These processes result ultimately in transformation of the initial 3D structure into a 2D adsorbed gold island whose area grows linearly with time [4]. On the other hand a homostructure, e.g., a 3D crystalline gold cluster deposited on an Au(111) surface, adsorbs epitaxially (in registry) with the substrate, exhibits enhanced stability and collapses at elevated temperatures via a dislocation mediated settling (DMS) mechanism, involving vacancies generated by surface dislocations in the deposited Au cluster. These novel atomic-scale mass transport and collapse mechanisms and the interplay between interfacial energetics and structure which they portray, pertain to a number of interfacial processes (e.g., deposited nanostructures, thin-film growth, annealing of damage, surface manipulations, and nanoscale lithography).

In the MD simulations we employed embedded atom method (EAM) potentials [5], for systems consisting of solid substrates containing N_d layers of dynamic atoms, exposing Ni(100) or Au(111) surfaces, with N_L atoms per layer. These dynamic substrates were positioned on top of N_s static layers with the corresponding geometry, and temperature was controlled via scaling of particle velocities at the bottom layer of the dynamic substrate. Periodic boundary conditions were imposed in directions parallel to the surface plane. Prior to simulations of the collapse processes, these systems, with deposited 3D gold clusters, were equilibrated at room temperature (300 K).

Earlier, we have shown [6] that contact between a metallic tip and a substrate (e.g., Ni or Au tips and Au or Ni surfaces) and subsequent slow retraction of the tip generate an elongated junction made of the softer metal (Au). Upon breaking of the contact a mound of gold is left on the surface, whose size an height increase when the retraction follows a slight indentation of the surface [6]. Indeed, gold mound formation via such a process has been demonstrated in recent STM experiments [3]. The 3D Au nanostructures which we investigated below were produced in this manner. We also mention recent investigations suggesting that metallic nanoclusters can be "soft-landed" on surfaces to form 3D deposited structures [7].

Au dot on a Ni(100) surface.—A sequence of atomic configurations illustrating collapse at 600 K of a 3D Au dot containing 154 atoms (with initially $n_1 = 97$, $n_2 = 29$, $n_3 = 17$, and $n_4 = 11$ in each of the layers of the deposited cluster; $N_d = 4$, $N_L = 800$, and $N_s = 3$) is shown in Fig. 1 and the corresponding kinetics of the process is described in Fig. 2. The core of the interfacial Au layer (layer 1 of the Au cluster) forms a (111) structure rotated by 30° with respect to the underlying Ni(100) surface (driven by the large lattice-constant mismatch between the two materials) and the structure close to the periphery of the interfacial layer is less ordered. The areal spreading of the Au interfacial layer is linear in time [Fig. 2(a)]. Furthermore, the radial atomic distributions in the resulting 2D Au island shown in Fig. 2(b) illustrate that atoms nearer to the middle of the island originated from higher layers in the 3D Au structure [i.e., layers more distant from the Ni(100) surface] while those closer to the periphery of the final 2D island correspond to atoms located initially in the interfacial layer of the Au cluster. This atomic distribution is inverted from the one that

0031-9007/94/73(4)/569(4)$06.00

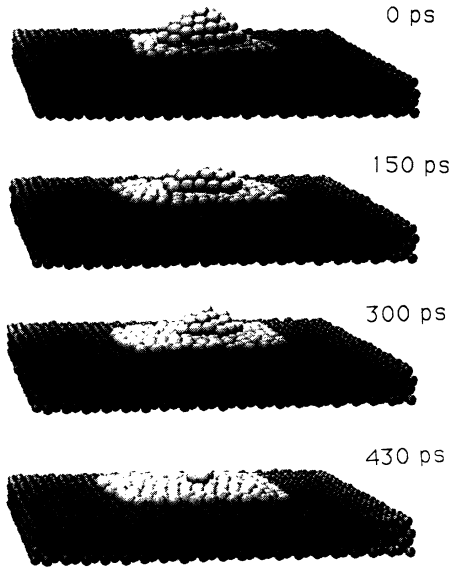

FIG. 1. Selected atomic configurations from simulations of the collapse of an Au cluster (light balls) on Ni(100) (dark balls) at 600 K.

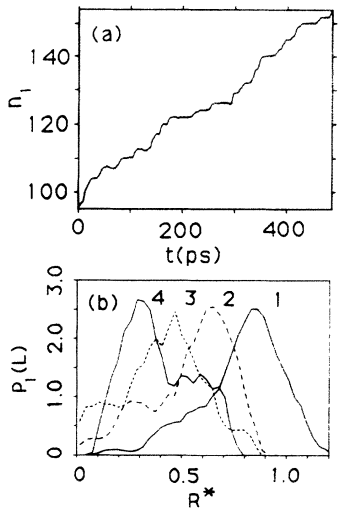

FIG. 2. (a) Number of particles (n_1) in the interfacial (bottom) layer of the adsorbed Au cluster (see Fig. 1), plotted versus time. (b) Radial distributions, $P_1(L)$, of Au atoms in the interfacial layer (i.e., the 2D Au island at the end of the collapse process, see bottom of Fig. 1), distinguished according to the layer of the cluster ($1 \leq L \leq 4$) from which they originated, plotted versus R^*, with the origin at the center of mass of the 2D patch. R^* is the distance of atoms from the origin, normalized by the mean radius of the island. $P_1(L)$ is normalized to unity for each L.

would have resulted if spreading occurred via diffusional transport and attachment of atoms from higher layers to the periphery of the interfacial, bottom, layer. Rather, it is a consequence of the SOSS mechanism where atoms at the periphery of layer $l + 1$ in the 3D Au cluster drop (embed) into the underlying lth layer inducing lateral radial outward atomic displacements in that layer. Such embedment sequences propagate from the top layer of the settling Au cluster downward, culminating in lateral spreading of the bottom (interfacial) Au layer on the Ni(100) surface.

Au dot on a Au(111) surface.—We have verified first that our simulations reproduce the $23 \times \sqrt{3}$ surface reconstruction observed on Au(111) [8], consisting of densification of the topmost layer via formation of a series of discommensurations, separating regions with fcc and faulted hcp stacking sequences, along the $[1\bar{1}0]$ direction. Furthermore, the presence of an adsorbed island causes local dereconstruction of the underlying gold layer.

Simulations of a Au cluster, similar to that described before, adsorbed epitaxially (in registry) on an Au(111) surface, have shown that while in the initial stages of the collapse embedding processes of similar nature to those discussed above take place, the process slowed down progressively, and continuation of the collapse (at least on time scales accessible to MD simulations) required heating to $T \gtrsim 800$ K. At this later stage a crossover to a dislocation mediated mechanism occurred (the aforementioned DMS), associated with shrinking of the areas of the topmost layers of the collapsing cluster and consequent increases in the distances between the peripheries of successive layers. These processes result in larger barriers for embedment (see below) thus suppressing the direct embedding mechanism. During the evolution of this system the DMS mechanism became particularly evident at the stage when the collapsing cluster consisted of two layers, an interfacial one and a small island on top; direct embedding occurred only when the top island migrated close to the periphery of the interfacial layer.

To further investigate the DMS mechanism we show in Fig. 3(a) the structure of a two-layer Au cluster consisting initially of a bottom interfacial layer and a top island containing 505 and 54 atoms, respectively, equilibrated initially at 300 K and then heated to 900 K, on a Au(111) substrate with $N_d = 2$ and $N_L = 1216$, together with atomic configurations illustrating structural evolution during a 30 ps interval [Figs. 3(b) and 3(d)]. Also included are fault contours [Fig. 3(c) corresponding to the structure in Fig. 3(b)], representing the displacements of atoms in the interfacial layer of the deposited cluster from their perfect fcc lattice positions. These contours illustrate reconstructed regions of fcc (C) and hcp (A) stacking (note that the hcp and discommensuration region on the left of the island indicate densification mainly along the $[1\bar{1}0]$ direction, and the ones on the right are along the $[1\bar{2}1]$ direction; short time scale dynamical fluctuations in the degree of perfection of the reconstruction patterns were observed throughout our simulations of finite gold islands at elevated temperatures).

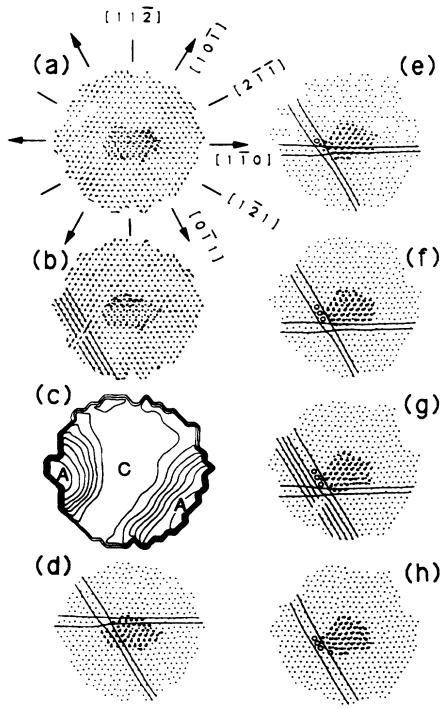

FIG. 3. Top views of atomic configurations [and short-time trajectories, in (a) and (b)] selected from simulations of a two-layer Au cluster adsorbed on a Au(111) surface, illustrating dislocation mediated settling (DMS). Only atoms of the adsorbed cluster are shown. The initial structure of the Au cluster, consisting of an interfacial layer [which exhibits a Au(111) reconstructed structure] and a second-layer island, is shown in (a). Formation of slip along the $[10\bar{1}]$ direction is shown in (b), along with corresponding fault contours in (c). (A and C denote hcp and fcc regions, respectively, separated by discommensuration regions. Mean displacements from perfect fcc positions are 0.4 Å in C and 1.5 Å in A, and the increment between contour lines is 0.15 Å.) Surface dislocations intersecting at the periphery of the second-layer island and formation of a vacancy are shown in (d), followed by a later configuration (e) where an embedded atom from the second layer filling the vacancy is indicated by an empty circle. Subsequent evolution leading to settling of three additional atoms into the interfacial layer is shown in (f)–(h). Thin guiding lines are drawn in (b) and (d)–(h).

Starting from the Au cluster shown in Fig. 3(a) the structural evolution shown in Figs. 3(b) and 3(d) involves generation of slip along the $[10\bar{1}]$ direction and an array of partial dislocations [9] [Fig. 3(b)] accompanied by formation of surface partial dislocations [Fig. 3(d)] with component Burgers vectors in the $[11\bar{2}]$ and $[2\bar{1}\bar{1}]$ directions (the total Burgers vector is along $[10\bar{1}]$). These dislocations are confined to the plane of the interfacial layer of the gold cluster [10], and get pinned at the periphery of the second layer island leading to formation of a vacancy in the interfacial layer [Fig. 3(d)]. Subsequently the vacancy gets filled by an atom originating from the second-layer island [see Fig. 3(e) where the embedded atom is marked by an empty circle].

Further evolution of the system, 260 ps later, during a 15 ps interval, illustrating dislocation mediated settling of three additional second-layer atoms, is shown in Figs. 3(e)–3(h). These atomic configurations illustrate movement of the dislocations [compare Figs. 3(e) and 3(d)], and climb of the dislocations via incorporation of two second-layer atoms [Fig. 3(f)]. Initiation of further slip along the $[10\bar{1}]$ direction and formation of surface partial dislocations are shown in Fig. 3(g). These processes resulted in annihilation of the dislocations leaving a vacancy in the interfacial layer. Finally the vacancy was filled by an atom displaced into it via settling of an additional atom from the top layer of the cluster [Fig. 3(h)].

The embedding energetics and structural properties of layers of the adsorbed Au clusters which are distant from the supporting substrate are similar in the two cases [i.e., on the Ni(100) and Au(111) substrates], while they differ markedly in the interfacial region, proximal to the surface, which governs the spreading propensity and rate. This is largely due to the difference in the surface energies of the two materials.

Results of constrained MD simulated annealing calculations (to 0 K), where certain degrees of freedom of a peripheral second-layer atom [the normal z coordinate, or (x, y) position] were constrained to a sequence (or "path") of specified values while relaxing the rest of the system, are shown in Fig. 4 for a two-layer gold cluster adsorbed on Au(111) (see left inset). Lateral detachment of an atom from the second-layer island involves a potential energy barrier of ~0.9 eV, and further displacements on the surface, along the path shown in the inset, require a smaller diffusion barrier (0.13 eV), with an increased barrier (0.16 eV) for "falling over the edge" to the underlying adsorbed layer [11]. Barriers for embedment of second-layer island atoms directly downward into the Au underlayer, calculated at several points along the above lateral path, are also shown in an inset to Fig. 4. Embedment of an atom near the edge of the second-layer island (point A) involves a barrier of 0.8 eV and is accompanied by spontaneous promotion of a neighboring atom from the interfacial layer of the structure to the layer above it, thus resulting in no net change in the number of atoms in these layers. On the other hand, embedments in locations distanced from the periphery of the island (points B, C, and D) involve smaller barriers and induce stress-relief sequences of outward atomic displacements occurring via slip, of a single atomic row, along specific directions, resulting in lateral expansion (spreading) of the interfacial layer [note that near the periphery of the interfacial layer, point D, atomic embedment from the layer above involves only a small barrier (0.02 eV) and is thus energetically more favorable than diffusion over the edge]. Consequently, diffusion and direct embedment processes are greatly suppressed by the aforementioned large detachment barrier.

Similar constrained MD calculations for the same Au cluster but adsorbed on a Ni(100) surface have shown that

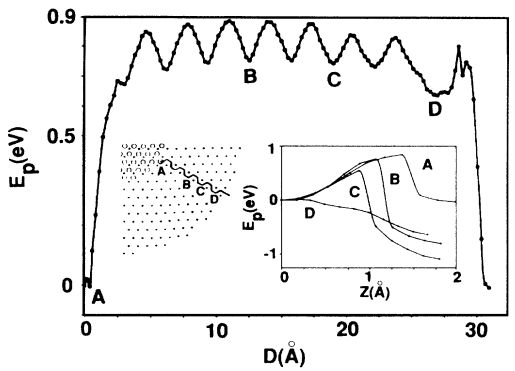

FIG. 4. Potential energy for lateral displacements of a gold atom starting from the periphery of a second-layer island of a two-layer Au cluster adsorbed on Au(111). The displacement D is along the path shown in the left inset (where a quadrant of the adsorbed cluster is shown). Potential energies versus normal displacement (z) for direct downward embedments from the second layer into the interfacial one, at locations corresponding to the indicated points on the path shown on the left, are given in the right inset. The origins of the energy and z scales were taken as those corresponding to the equilibrium configurations before displacements.

detachment of an Au atom to a distance of ~1 Å from the periphery of the second layer island (involving a barrier of ~0.5 eV), is accompanied by a spontaneous incorporation into the interfacial layer leading to spreading.

We conclude that the collapse of a heterostructure, such as a 3D Au cluster adsorbed on Ni(100) can occur via a settling mechanism (SOSS), involving local atomic incorporation (embedment into underlayers). These processes are driven by the resulting gain in interfacial cohesion and are aided by the large lattice mismatch between the two materials, which reduces the interfacial frictional resistance to stress relief via outward lateral atomic displacements, resulting in spreading. On the other hand for Au clusters adsorbed on Au(111) the much reduced energetic driving force, coupled with high interfacial friction due to the epitaxial structure of the interface between the deposited cluster and the substrate, result in higher stability compared to that of Au/Ni(100). Here collapse at elevated temperatures is mediated by a settling mechanism involving spontaneous generation and propagation of surface dislocations (DMS). While diffusion has been invoked in interpretation of experimental results pertaining to collapse of nanostructures on surfaces, no direct evidence for diffusion events was given [2]; this does not preclude diffusion to the edge in the case of deposited single atoms, where there is no detachment barrier, or of very small clusters, as observed in FIM experiments [11(a)]. The alternative collapse mechanisms which we found may dominate in certain ranges of sizes and temperatures in the systems studied by us as well as in other materials [12].

Research supported by the U.S. Department of Energy and by the AFOSR. Computations were performed on Cray computers at the National Energy Research Supercomputer Center, Livermore, CA.

[1] See articles in *Atomic and Nanometer-Scale Modification of Materials: Fundamentals and Applications*, edited by P. Avouris (Kluwer, Dordrecht, 1993).

[2] R.C. Jaklevic and L. Ellie, Phys. Rev. Lett. **60**, 120 (1988); Y.Z. Li *et al.*, Appl. Phys. Lett. **54**, 1424 (1989); R. Emch *et al.*, J. Appl. Phys. **65**, 79 (1989); D.G. Walmsley *et al.*, Nanost. Mater. **3**, 245 (1993); T. Michely *et al.*, Surf. Sci. Lett. **230**, L135 (1990); H.J. Mamin *et al.*, Phys. Rev. Lett. **65**, 2418 (1990); and J. Vac. Sci. Technol. B **9**, 1398 (1991), where stability and minimal diffusion, even at elevated temperatures, are discussed; D.R. Peale and B.H. Cooper, J. Vac. Sci. Technol. A **10**, 2210 (1992); and B.H. Cooper *et al.* in *Evolution of Surface and Thin Film Microstructure*, edited by H.A. Atwater *et al.* (MRS, Pittsburgh, 1993), p. 37, where linear in time collapse of gold features on a gold surface in air, and enhanced stability of such features under clean conditions, were observed.

[3] J.J. Pascual *et al.*, Phys. Rev. Lett. **71**, 1852 (1993).

[4] U. Landman and W.D. Luedtke, Appl. Surf. Sci. **60/61**, 1 (1992).

[5] With the parameterization given in J.B. Adams *et al.*, J. Mater. Res. Soc. **4**, 102 (1989).

[6] U. Landman *et al.*, Science **248**, 454 (1990); W.D. Luedtke and U. Landman, J. Vac. Sci. Technol. B **9**, 414 (1991).

[7] H.-P. Cheng and U. Landman, J. Phys. Chem. **98**, 3527 (1994).

[8] For recent experimental studies see (a) U. Harten *et al.*, Phys. Rev. Lett. **54**, 2619 (1985); (b) Ch. Woll *et al.*, Phys. Rev. B **39**, 7988 (1989); (c) J.V. Barth *et al.*, Phys. Rev. B **42**, 9307 (1990); (d) A.R. Sandy *et al.*, Phys. Rev. B **43**, 4667 (1991).

[9] The slip and consequent strain relief involving surface dislocations, involved atoms occupying bridge sites of the underlying substrate surface layer [see Figs. 3(b) and 3(c) where slip occurs along fault contours corresponding to bridge sites]. However, the degree to which such bridge-site fault directions are easy slip directions depends on their orientation relative to the substrate and on which bridge sites are occupied.

[10] These surface dislocations are the 2D analogs of the known dissociation of the [110] dislocation in fcc crystals [see D. Hull, *Introduction to Dislocations* (Pergamon, Oxford, 1975)]. For a discussion in the context of reconstruction of Au(111) and Pt(111) see Ref. 8(c); D.D. Chambliss *et al.*, Phys. Rev. Lett. **66**, 1721 (1991); M. Bott *et al.*, Phys. Rev. Lett. **70**, 1489 (1993).

[11] See reviews by (a) G. Ehrlich, Appl. Phys. A **55**, 403 (1992); (b) M.G. Lagally, Phys. Today **46**, No. 11, 24 (1993).

[12] H. Hakkinen and U. Landman, Phys. Rev. Lett. **71**, 1023 (1993).

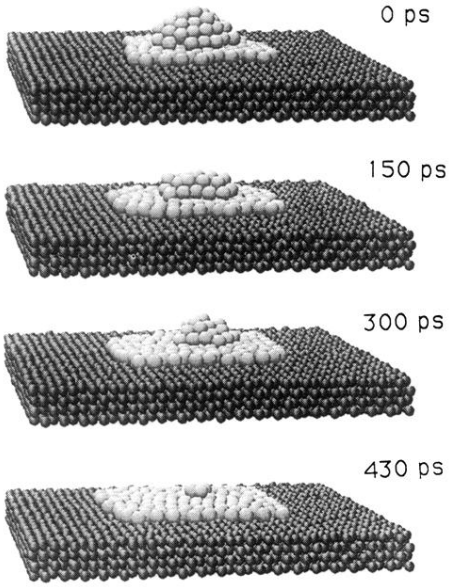

FIG. 1. Selected atomic configurations from simulations of the collapse of an Au cluster (light balls) on Ni(100) (dark balls) at 600 K.

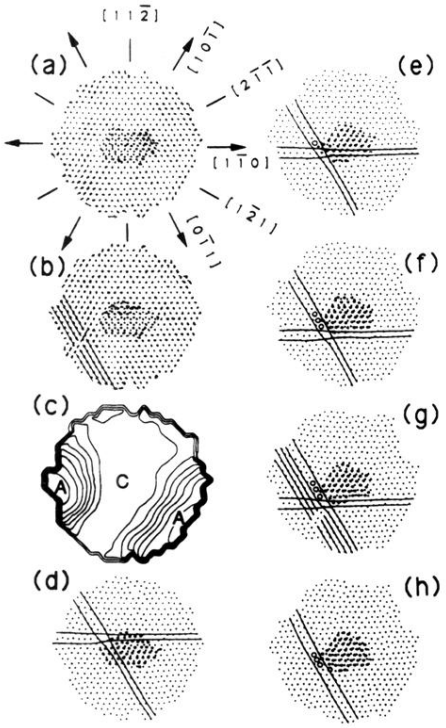

FIG. 3. Top views of atomic configurations [and short-time trajectories, in (a) and (b)] selected from simulations of a two-layer Au cluster adsorbed on a Au(111) surface, illustrating dislocation mediated settling (DMS). Only atoms of the adsorbed cluster are shown. The initial structure of the Au cluster, consisting of an interfacial layer [which exhibits a Au(111) reconstructed structure] and a second-layer island, is shown in (a). Formation of slip along the $[10\bar{1}]$ direction is shown in (b), along with corresponding fault contours in (c). (A and C denote hcp and fcc regions, respectively, separated by discommensuration regions. Mean displacements from perfect fcc positions are 0.4 Å in C and 1.5 Å in A, and the increment between contour lines is 0.15 Å.) Surface dislocations intersecting at the periphery of the second-layer island and formation of a vacancy are shown in (d), followed by a later configuration (e) where an embedded atom from the second layer filling the vacancy is indicated by an empty circle. Subsequent evolution leading to settling of three additional atoms into the interfacial layer is shown in (f)–(h). Thin guiding lines are drawn in (b) and (d)–(h).